


Topological transitions in electronic spectra: Crossover between Abrikosov and Josephson vortices

A. V. Samokhvalov ^{1,2}, V. D. Plastovets ^{1,2,3} and A. S. Mel'nikov^{1,2,3}

¹*Institute for Physics of Microstructures, Russian Academy of Sciences, GSP-105, 603950 Nizhny Novgorod, Russia*

²*Lobachevsky State University of Nizhni Novgorod, 603950 Nizhni Novgorod, Russia*

³*Sirius University of Science and Technology, 1 Olympic Avenue, 354340 Sochi, Russia*

 (Received 18 June 2020; revised 11 September 2020; accepted 15 October 2020; published 2 November 2020)

The electronic structure of a vortex line trapped by a planar defect in a type-II superconductor is analyzed within the quasiclassical approach of the Bogoliubov–de Gennes theory. The normal reflection of electrons and holes at the defect plane results in the topological transition in the spectrum and formation of a type of quasiparticle state skipping or gliding along the defect. This topological transition appears to be a hallmark of the initial stage of the crossover from the Abrikosov to the Josephson vortex type revealed in the specific behavior of the quantized quasiparticle levels and density of states. The increase in the resulting hard and soft gaps affects the vortex mobility along the defect plane and the splitting of the zero-bias anomaly in the tunneling spectral characteristics.

DOI: [10.1103/PhysRevB.102.174501](https://doi.org/10.1103/PhysRevB.102.174501)

I. INTRODUCTION

The most general definition of different vortex-type solutions for the order parameter in superconducting and superfluid systems is based on the calculation of the so-called circulation of the gradient of the order parameter phase around the line of singularity. Provided this circulation equals 2π , we get a singly quantized vortex. The particular structure of the order parameter and magnetic field distributions strongly depends then on the specific system. In a homogeneous isotropic superconductor the vortex solution possessing a cylindrical symmetry is well known as an Abrikosov vortex [1], while the presence of any anisotropy or inhomogeneity can strongly deform this vortex line in the plane x - y perpendicular to its axis (see Fig. 1). An extreme example of such an anisotropic solution which does not even possess the normal core can be realized for a vortex pinned at the Josephson junction [2]. Such quasi-one-dimensional vortices are also called Josephson vortices [see Fig. 1(a)] and are known to play an important role in magnetic and transport properties of layered and nanostructured systems. Provided the junction critical current density j_c is much smaller than the depairing current density

$$j_d = c\Phi_0/12\sqrt{3}\pi^2\lambda^2\xi, \quad (1)$$

the Josephson penetration depth

$$\lambda_J = \sqrt{c\Phi_0/16\pi^2j_c\lambda} \quad (2)$$

appears to be much larger than the London penetration depth λ . Here $\Phi_0 = \pi\hbar c/e$ is the magnetic flux quantum and ξ is the superconducting coherence length. Clearly, changing the electron transparency of the junction, one can get a variety of intermediate vortex states corresponding to a crossover from the Josephson to the Abrikosov vortex [3–5]. This situation with the intermediate transparencies naturally appears in many superconducting systems studied in experiments,

e.g., in superconductors with twinning planes [6], low-angle grain boundaries [7,8], or other types of defects [9–11]. An appropriate theoretical treatment needed, for instance, for the interpretation of the experimental data on the magnetic field distribution can be well developed on the basis of the Ginzburg-Landau theory. Indeed, using a general expression [12] for the critical current I_c across the junction with a cross-section area S ,

$$I_c = j_c S = \pi \Delta_0 / 2eR_N, \quad (3)$$

and the relation between the contact resistance and the angle-averaged transmission probability of the barrier \mathcal{T} ,

$$R_N^{-1} = k_F^2 S (2e^2/\hbar) \mathcal{T}, \quad (4)$$

we derive the simple relation

$$\lambda_J^2 = \lambda \xi / 12\pi^2 \mathcal{T}. \quad (5)$$

It is natural that the Josephson length λ_J grows if the transmission probability of the barrier \mathcal{T} decreases. To satisfy the relation $\lambda_J \gg \lambda$, the barrier transparency should be small enough: $\mathcal{T} \ll \mathcal{T}_\lambda = 1/12\pi^2\kappa \ll 1$, where $\kappa = \lambda/\xi$ is the Ginzburg-Landau parameter. As the probability of electron transmission through the barrier grows above \mathcal{T}_λ the changes in the structure of the order parameter are controlled by the relation between the Josephson length λ_J , the London penetration depth λ , and the coherence length ξ . Keeping in mind type-II superconductors, we should take $\xi \lesssim \lambda$. When the current density $j(r)$ in the vortex core ($r \lesssim \xi$) becomes of order of the depairing one j_d , the length l of the core along the defect can be estimated from the continuity of currents flowing parallel and perpendicular to the defect within the core [3]: $lj_c \sim j_d \xi$, whence $l \sim j_d \xi / j_c \sim \lambda_J^2 / \lambda$. The case $\mathcal{T} \gtrsim \mathcal{T}_\lambda$ ($\xi < l \lesssim \lambda \sim \lambda_J$) corresponds to the limit of strong Josephson coupling with $j_c \gtrsim j_d / \kappa$, and we can no longer consider the solution in the form of a core-free Josephson vortex having

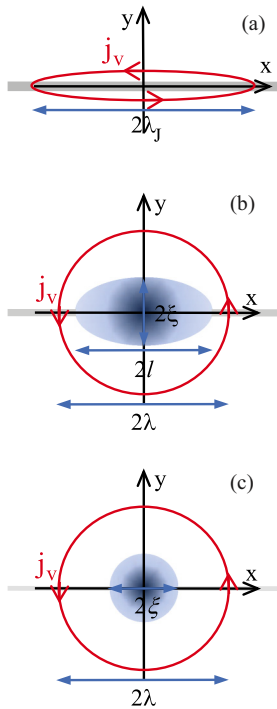


FIG. 1. Vortex pinned by a planar defect positioned in the $y = 0$ plane for several values of the barrier transparency \mathcal{T} : (a) the Josephson vortex for weak coupling ($l \gg \lambda_J \gg \lambda$) for $\mathcal{T} \ll \mathcal{T}_\lambda$, (b) the Abrikosov-like vortex for strong coupling ($l \sim \lambda_J \sim \lambda$) for $\mathcal{T} \sim \mathcal{T}_\lambda$, and (c) the Abrikosov vortex ($l \sim \xi$) for $\mathcal{T} \sim \mathcal{T}_\xi$. The region of the vortex core is shown in gray. The current streamline around the vortex in the x - y plane perpendicular to its axis in the z direction is shown by a solid red line.

the size of the order λ_J . Instead, we get the crossover to the Abrikosov-like vortex having a strongly deformed anisotropic core ($l \times \xi$), where the superconducting order parameter is suppressed [see Fig. 1(b)]. The distributions of the magnetic field and circular screening currents outside the core ($r \gg l, \xi$) approach now the ones for the Abrikosov vortex in a uniform superconductor. In the case of the extremely strong Josephson coupling $\mathcal{T} \gtrsim \mathcal{T}_\xi = 1/12\pi^2$ ($l \lesssim \xi$) the anisotropy of the vortex core becomes negligible, and at this initial stage of the crossover [see Fig. 1(c)] the order parameter profile of the Abrikosov vortex core is almost insensitive to the defect.

Despite the general correctness of the above qualitative picture, there exist several important physical issues which definitely cannot be described within the phenomenological model and demand a more careful microscopic consideration. This statement surely relates to the scanning tunneling microscopy (STM) and spectroscopy data which provide detailed spatially resolved excitation spectra [13–17] and also to the problem of the vortex dynamics and dissipation [18–23]. In the latter case the crossover from the Abrikosov to the Josephson vortex is particularly important since it is accompanied by the disappearance of the normal vortex core which provides the dominating contribution to the dissipation and resulting vortex viscosity [7]. It is the goal of the present work to develop a theoretical description of the changes in the electronic structure of the pinned vortex core which occur during

the crossover between the Abrikosov and Josephson vortices and unveil a nontrivial topological nature of this vortex core transformation.

Considering the microscopic theory, one should take into account the behavior of the subgap fermionic states bound to the Abrikosov vortex core which are known to determine both the structure and dynamics of vortex lines in the low-temperature limit (see Ref. [18] for details). These subgap states are known to form the so-called anomalous spectral branch crossing the Fermi level. For well-separated vortices the behavior of the anomalous branches can be described by the Caroli–de Gennes–Matricon (CdGM) theory [24]: For each individual vortex the energy $\varepsilon_{\text{CdGM}}(\mu)$ of subgap states varies from $-\Delta_0$ to $+\Delta_0$ as one changes the angular momentum μ defined with respect to the vortex axis. Here Δ_0 is the superconducting gap value far from the vortex axis. At small energies $|\varepsilon| \ll \Delta_0$ the spectrum is a linear function of μ : $\varepsilon_{\text{CdGM}}(\mu) \simeq -\mu\hbar\omega_0$, where $\hbar\omega_0 \approx \Delta_0/k_F\xi = \Delta_0^2/2E_F \ll \Delta_0$ is the interlevel spacing, $\xi = \hbar V_F/\Delta_0$, and $p_F = \hbar k_F$, V_F , and E_F are Fermi momentum, velocity, and energy, respectively. We use here the quasiclassical approach, which is valid if the characteristic size ξ of the vortex core is much larger than the Fermi wavelength of quasiparticles $\lambda_F = 2\pi/k_F$. As a result, the quasiparticles propagate along almost straight classical trajectories which are characterized by the direction of the quasiparticle momentum $\mathbf{p}_F = \hbar k_\perp (\cos\theta_p \mathbf{e}_x + \sin\theta_p \mathbf{e}_y) + \hbar k_z \mathbf{e}_z$ and the impact parameter $b = -\mu/k_\perp$. The subgap bound states of quasiparticles form at these straight trajectories due to the Andreev reflection [25] from the gap profile inside the vortex core. Neglecting the quantization of the angular momentum μ , one can get the anomalous spectral branch crossing the Fermi level at $\mu = 0$ for all orientations of the momentum \mathbf{p}_F . Thus, in the μ - \mathbf{p}_F space we obtain a Fermi surface for excitations localized within the vortex core (see Ref. [26] for review). For fixed values of the energy ε and the momentum projection at the vortex axis $\hbar k_z$ we can define a quasiclassical orbit in the plane μ - θ_p : $\mu(\theta_p) = -\varepsilon/\hbar\omega_0$. Each point in this orbit corresponds to a straight trajectory passing through the vortex core, which is determined by the impact parameter b and the angle θ_p (Fig. 2). For an isotropic vortex core a θ_p dependence of the energy ε is lacking, and isoenergetic lines form open orbits shown by dotted lines in Fig. 3(a). The two-dimensional (2D) quantum mechanical nature of the quasiclassical solution can be restored if one takes into account the precession of the quasiparticle trajectories which is triggered by the small deviations from the exact backscattering in the Andreev reflection processes and described by the Hamilton equation $\hbar\partial\theta_p/\partial t = \partial\varepsilon/\partial\mu$. For a free Abrikosov vortex the straight trajectories precess (or just rotate) around the vortex center by the angle 2π (see Ref. [18]).

Any additional normal scattering process should modify the behavior of the anomalous spectral branch. Such modification can be noticeable even for impurity atoms introduced in a vortex core [21] and becomes much more pronounced provided we consider a vortex pinned by a normal metal [27,28] or an insulating [29–32] columnar defect of the size $R \ll \xi$, far exceeding the Fermi wavelength. In the last case the scattering at the defect is responsible for the opening of the minigap $\varepsilon_0 \sim \Delta_0 R/\xi$ in the spectrum of localized states and

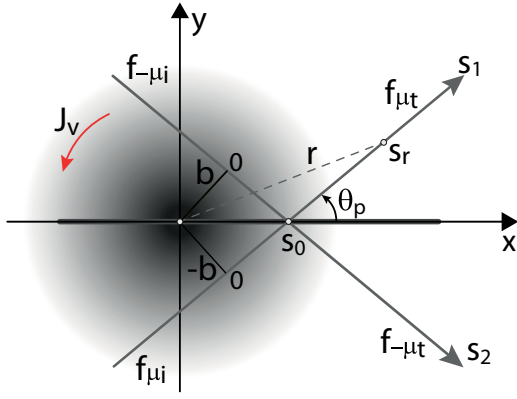


FIG. 2. Specular reflection of quasiclassical trajectories s_1 and s_2 with opposite values of the angular momentum $\mu = \pm k_{\perp}|b|$ at the defect in the plane $y = 0$. The region of the vortex core is shown in gray. The red arrow shows the direction of the supercurrent in the vortex.

resulting suppression of the dissipation at low temperatures $T \ll \varepsilon_0$ [18,33]. For a vortex approaching a flat or curved sample boundary, an appropriate spectrum transformation was studied in Refs. [34–37]. Change in the anomalous spectral branch is accompanied by the changes in the topology of quasiclassical orbits in the μ - θ_p plane. Such topological transitions in quasiparticle spectra of vortex systems are similar to the well-known Lifshitz transitions which occur in the

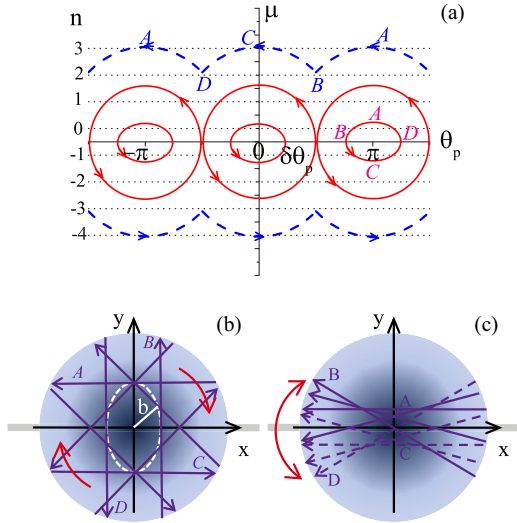


FIG. 3. (a) Quasiparticle orbits (8) in the μ - θ_p plane corresponding to different energy levels n shown schematically by red solid (closed orbits) and blue dashed (open orbits) lines. For reference, dotted lines show the orbits for a single Abrikosov vortex in the absence of a barrier. Arrows show the direction of the quasiparticle trajectory precession along the orbit. Also shown is the precession of the quasiparticle trajectory for (b) open and (c) closed orbits. The trajectories A, B, C, and D correspond to the appropriate points at the orbits indicated in Fig. 3(a). Solid and dashed trajectories correspond to the cases $\mu \geq 0$ and $\mu \leq 0$, respectively. The region of the vortex core is shown in gray. The direction of the trajectory precession is shown by red arrows.

band spectra of metals [38,39]. The generic examples of such transitions in vortex matter including the opening of the closed segments of the orbits in the μ - θ_p plane or merging and reconnection of the different segments via the Landau-Zener tunneling have been previously studied in Refs. [36,40,41]. The basic properties of vortex matter such as pinning and transport characteristics, heat transport in the vortex state, and peculiarities of the local density of states should be strongly affected by these changes in the topology of the subgap spectral branches.

To elucidate our main findings we start from the simplified qualitative picture illustrating the effect of the barrier on the quasiparticle subgap states. Our idea is that the scattering at the plane defect with some finite transparency \mathcal{T} can strongly affect the quasiparticle trajectory precession preventing the trajectory from rotating by the full angle 2π . This destruction of the trajectory rotation around the vortex center should be accompanied by the changes in the topology of the quasiclassical orbits and qualitative modification of the quasiparticle spectrum. We restrict ourselves to situations when the barrier is rather weak, assuming $\mathcal{T}_{\xi} \lesssim \mathcal{T} < 1$, and focus on the modification of the anomalous energy branches which occurs in a vortex pinned by a planar defect due to the quasiparticle normal reflection at the defect boundary. First, considering the specular reflection of the quasiclassical trajectories at the plane defect in Fig. 2, one can clearly see that the scattering couples the wave functions with the opposite angular momenta $\pm\mu$. Overlapping of these wave functions transforms the quasiclassical spectrum, resulting in the modification of the topology of isoenergetic lines in the μ - θ_p plane. Phenomenologically, one can describe this coupling by a standard two-level problem, which yields the secular equation

$$(\varepsilon - \varepsilon_{\mu})(\varepsilon - \varepsilon_{-\mu}) \approx [V_{\text{gap}}(\theta_p)]^2, \quad (6)$$

where ε_{μ} denotes the anomalous spectral branch for a linear trajectory passing through the core of a free vortex. The scattering obviously cannot couple the trajectories with $\theta_p = 0, \pm\pi$, which are parallel to the defect plane. Considering now the limit of small angles θ_p , one can expect that even for the barriers with rather good transparency \mathcal{T} the tunneling probability should vanish in this angular interval. The splitting of the energy levels around $\varepsilon = 0$ should originate from the superconducting phase difference ϕ at the ends of the incident $f_{-\mu i}$ ($f_{\mu i}$) and reflected $f_{\mu t}$ ($f_{-\mu t}$) trajectories (see Fig. 2). This phase difference ϕ equals $\pm(\pi - 2\theta_p)$. Using now a standard expression for the subgap Andreev state energy in a one-dimensional Josephson junction [42], we find

$$\varepsilon = \pm \Delta_0 \sqrt{1 - \mathcal{T} \sin^2(\phi/2)} \simeq \pm \Delta_0 \sqrt{1 - \mathcal{T} + \mathcal{T}\theta_p^2}. \quad (7)$$

This energy splitting gives us the estimate for the coupling coefficient in the above two-level problem (6): $V_{\text{gap}}(\theta_p) \sim \Delta_0 \theta_p$ for a planar defect with a high transparency $\mathcal{T} \rightarrow 1$.

As a result, one obtains a set of quasiclassical orbits in μ - θ_p space

$$\mu(\theta_p) = \pm \frac{1}{\hbar\omega_0} \sqrt{\varepsilon^2 - \Delta_0^2 \theta_p^2}. \quad (8)$$

These orbits (8) corresponding to the precession of the quasiparticle trajectory are schematically shown in Fig. 3(a). For

low-energy levels one can clearly observe the formation of closed orbits near the degeneracy points $\theta_p = 0, \pm\pi$, which are separated by the prohibited angular domains centered at $\theta_p = \pm\pi/2$, where the precession of the trajectory appears to be forbidden [Fig. 3(c)]. These closed trajectories form from the open ones through a topological transition. The closed orbits are nothing but skipping (or gliding) quasiparticle states formed due to the scattering at the defect plane. The quasiparticle momenta for these states are almost parallel to the plane of the defect while their wave functions decay along the trajectory direction at the superconducting coherence length. The corresponding discrete subgap energy levels of quasiparticles can be obtained from the semiclassical Bohr-Sommerfeld quantization rule for canonically conjugate variables μ and θ_p [43,44],

$$\Sigma(\varepsilon) = \int_0^{2\pi} \mu(\varepsilon, \theta_p) d\theta_p = 2\pi(n + \beta), \quad (9)$$

where n is an integer, 2π is the period of $\mu(\theta_p)$, and β is of the order unity. Applying the Bohr-Sommerfeld rule (9) to the closed paths in μ - θ_p space, we obtain the spectrum in the form

$$\varepsilon_n^2 = \frac{\Delta_0^3}{E_F}(n + \beta), \quad (10)$$

which is dramatically different from the CdGM spectrum $\varepsilon_n = \hbar\omega_0(n + 1/2)$ and is reminiscent of the square-root quantization of the quasiparticle spectra in different types of nodal problems (like graphene [45,46] or d -wave superconductors in magnetic fields [47]). Note that this draft estimate of the energy of low subgap spectrum levels appears to be in good agreement with the explicit expression for the energy levels (35) on the basis of the full quantitative description in Sec. III. The minigap $\varepsilon_0 \simeq \Delta_0\sqrt{\Delta_0/E_F}$ determined by Eq. (10) far exceeds the CdGM interlevel spacing $\hbar\omega_0$. This minigap increase obviously manifests the partial suppression of the spectral flow, which should give origin to all the dissipation phenomena inside the vortex core during its motion. In this sense this spectrum change can be viewed as a precursor to the crossover to the Josephson vortex where all the subgap quasiparticle levels are repelled from the Fermi energy to the gap value Δ_0 . On the other hand, the limit of the moderate barrier strength studied here provides a possibility to observe a different type of vortex core with the peculiar quantization rule arising from the splitting of the orbit segments in the μ - θ_p plane. This splitting destroys the trajectory precession in the whole angular interval $0 < \theta_p < 2\pi$, changing thus the topology of the quasiclassical orbits. The precession region $|\theta_p| \leq \delta\theta_p$ expands with an increase of the energy level n . As a result, for rather high levels the prohibited angular domains shrink, the precession over the full region $0 \leq \theta_p \leq 2\pi$ is restored, and we get the crossover to a CdGM type of spectrum $\varepsilon_n \sim n$.

The paper is organized as follows. In Sec. II we introduce the basic equations used for the spectrum calculation. In Sec. III we study the quasiparticle spectrum transformation for a singly quantized vortex pinned at the planar defect and discuss the consequences for the vortex dynamics. Section IV is devoted to the analysis of the peculiarities of the local density of states for a vortex pinned at the defect. We summarize our results in Sec. V.

II. BASIC EQUATIONS

Hereafter we consider a planar defect in the plane $y = 0$ as a δ -function repulsive potential for quasiparticles, i.e., $V(y) = H\delta(y)$. The magnetic field $\mathbf{B} = B\mathbf{z}_0$ is assumed to create a single quantum vortex line parallel to the z axis trapped inside the attractive potential well within the defect [48]. The vortex center defined as a point of the order parameter phase singularity is positioned at the point $x = y = 0$.

We assume the system to be homogeneous along the z axis; thus the $\hbar k_z$ projection of the momentum is conserved. The quantum mechanics of quasiparticle excitations in a superconductor is governed by the two-dimensional Bogoliubov–de Gennes (BdG) equations for particlelike (u) and holelike (v) parts of the two-component quasiparticle wave functions $(u(\mathbf{r}), v(\mathbf{r}))^T \exp(ik_z z)$:

$$-\frac{\hbar^2}{2m}(\nabla^2 + k_\perp^2)u + \Delta(\mathbf{r})v = \varepsilon u, \quad (11a)$$

$$\frac{\hbar^2}{2m}(\nabla^2 + k_\perp^2)v + \Delta^*(\mathbf{r})u = \varepsilon v. \quad (11b)$$

Here $\nabla = \partial_x \mathbf{x}_0 + \partial_y \mathbf{y}_0$, $\mathbf{r} = (x, y)$ is a radius vector in the plane perpendicular to the magnetic field direction, $\Delta(\mathbf{r})$ is the gap function, and $k_\perp^2 = k_F^2 - k_z^2$.

The potential barrier is assumed to be partially transparent for electrons and the appropriate boundary conditions for wave function $\hat{\Psi}(x, y) = (u(\mathbf{r}), v(\mathbf{r}))^T$ at $y = 0$ read [49]

$$\hat{\Psi}(x, 0+) = \hat{\Psi}(x, 0-) = \hat{\Psi}_0, \quad (12a)$$

$$\partial_y \hat{\Psi}(x, 0+) - \partial_y \hat{\Psi}(x, 0-) = 2k_\perp Z \hat{\Psi}_0, \quad (12b)$$

where the dimensionless barrier strength $Z = H/\hbar V_\perp$ ($mV_\perp = \hbar k_\perp$) defines the transmission $\mathcal{T} = 1/(1 + Z^2)$ and reflection $Z^2/(1 + Z^2)$ coefficients in the normal state. For an extremely weak barrier ($\mathcal{T} \gtrsim \mathcal{T}_\xi$) we can neglect the anisotropy of the order parameter $\Delta(\mathbf{r})$ within the vortex core and assume that

$$\Delta(\mathbf{r}) = \Delta_0 \delta_v(r) e^{i\theta}, \quad r = \sqrt{x^2 + y^2}, \quad (13)$$

where (r, θ) is a polar coordinate system. Here $\delta_v(r)$ is a normalized order parameter magnitude for a vortex centered at $r = 0$ such that $\delta_v(r) = 1$ for $r \rightarrow \infty$. Following the procedure described in [35,36,41] (see the Appendix for details), we introduce the momentum representation

$$\hat{\Psi}(\mathbf{r}) = \frac{1}{(2\pi\hbar)^2} \int_{-\infty}^{+\infty} d^2\mathbf{p} e^{i\mathbf{p}\mathbf{r}/\hbar} \hat{\psi}(\mathbf{p}), \quad (14)$$

where $\mathbf{p} = |\mathbf{p}|(\cos \theta_p, \sin \theta_p) = p\mathbf{p}_0$. The unit vector \mathbf{p}_0 parametrized by the angle θ_p defines the trajectory direction in the x - y plane. We assume that our solutions correspond to the momentum absolute values p close to the value $\hbar k_\perp$: $p = \hbar k_\perp + q$ ($|q| \ll \hbar k_\perp$). Within the quasiclassical approach, the wave function in the momentum representation assumes the form

$$\hat{\psi}(\mathbf{p}) = \frac{1}{k_\perp} \int_{-\infty}^{+\infty} ds e^{i(k_\perp - |\mathbf{p}|/\hbar)s} \hat{\psi}(s, \theta_p), \quad (15)$$

where s is a coordinate along a quasiclassical trajectory, which is a straight line along the direction of the quasiparticle momentum. Finally, the wave function $\hat{\Psi}(\mathbf{r})$ in the real space

$\mathbf{r} = r(\cos \theta, \sin \theta)$ is expressed in the following way via the slowly varying functions $\hat{\psi}(s, \theta_p)$ defined at the trajectory:

$$\hat{\Psi}(r, \theta) = \int_0^{2\pi} e^{ik_{\perp}r \cos(\theta_p - \theta)} \hat{\psi}(r \cos(\theta_p - \theta), \theta_p) \frac{d\theta_p}{2\pi}. \quad (16)$$

The solution (16) cannot be characterized by a definite angular momentum μ because the partial transparency of the barrier makes it possible to couple four quasiclassical rays at the plane defect. As a result, the angular harmonics $f_{\pm\mu i}$ and $f_{\pm\mu t}$ (see Fig. 2) with opposite momenta μ and $-\mu$ become interacting, contrary to the case considered in [29]. To account for this four-wave coupling, we follow Ref. [50] and introduce the angular momentum expansion for the solution (16),

$$\hat{\psi}(s, \theta_p) = \sum_{\mu} e^{i\mu\theta_p + i\hat{\sigma}_z\theta_p/2} \hat{f}_{\mu}(s), \quad (17)$$

where the discreteness of the angular momentum $\mu = n + 1/2$ (n is an integer) arises from the obvious condition that the wave function (17) is single valued. The function $\hat{f}_{\mu}(s)$ satisfies the Andreev equation along the quasiclassical trajectory with the impact parameter $b = -\mu/k_{\perp}$,

$$-i\hbar V_{\perp} \hat{\sigma}_z \partial_s \hat{f}_{\mu} + \hat{\Delta}_b(s) \hat{f}_{\mu} = \varepsilon \hat{f}_{\mu}, \quad (18)$$

where

$$\hat{\Delta}_b(s) = \hat{\sigma}_x \text{Re} D_b(s) - \hat{\sigma}_y \text{Im} D_b(s) \quad (19)$$

is the gap operator, $\hat{\sigma}_i$ are the Pauli matrices, and the expression for the order parameter $\Delta = D_b(s) e^{i\theta_p}$ around the vortex in (s, θ_p) variables

$$D_b(s) = \Delta_0 \frac{\delta_v(\sqrt{s^2 + b^2})}{\sqrt{s^2 + b^2}} (s + ib) \quad (20)$$

can be obtained from (13), taking into account the evident relations

$$\begin{aligned} x &= s \cos \theta_p - b \sin \theta_p, & y &= s \sin \theta_p + b \cos \theta_p, \\ x \pm iy &= (s \pm ib) e^{\pm i\theta_p}. \end{aligned}$$

Note that the impact parameter b and the trajectory orientation angle θ_p are two independent quantities which parametrize the linear quasiclassical trajectory in the x - y plane.

A. General solution

To find the solution of Eqs. (18)–(20) we can use the results of Ref. [35]. For low energies ($\mu \ll k_{\perp} \xi$) we take the function

\hat{f}_{μ} as a sum

$$\hat{f}_{\mu} = \begin{pmatrix} u_{\mu} \\ v_{\mu} \end{pmatrix} = c_{\mu 1} \hat{G}_{\mu 1} + c_{\mu 2} \hat{G}_{\mu 2} \quad (21)$$

of the two linearly independent solutions

$$\hat{G}_{\mu 1} = e^{i\hat{\sigma}_z \pi/4} \left(e^{-|K_{\mu}(s)|} - i \text{sgn}(s) \frac{\gamma_{\mu}}{2} \hat{\sigma}_z e^{|K_{\mu}(s)|} \right) \hat{\lambda}, \quad (22a)$$

$$\hat{G}_{\mu 2} = e^{i\hat{\sigma}_z \pi/4} e^{-|K_{\mu}(s)|} \hat{\sigma}_z \hat{\lambda}, \quad (22b)$$

where $\hat{\lambda} = (1, 1)^T$,

$$K_{\mu}(s) = \frac{k_F}{k_{\perp} \xi} \int_0^s dt \frac{t \delta_v(\sqrt{t^2 + b^2})}{\sqrt{t^2 + b^2}}, \quad (23)$$

$$\Lambda_{\mu} = \frac{2k_F}{k_{\perp} \xi} \int_0^{\infty} ds e^{-2K_{\mu}(s)}, \quad (24)$$

$$\gamma_{\mu} = \frac{\Delta_{\mu}}{\Delta_0} (\varepsilon_{\mu} - \varepsilon), \quad (25)$$

with

$$\varepsilon_{\mu} = -\frac{2\Delta_0 k_F \mu}{k_{\perp}^2 \xi \Lambda_{\mu}} \int_0^{\infty} ds \frac{\delta_v(\sqrt{s^2 + b^2})}{\sqrt{s^2 + b^2}} e^{-2K_{\mu}(s)} \quad (26)$$

the CdGM excitation spectrum. Here $\xi = \hbar V_F / \Delta_0$ is the coherence length (V_F is the Fermi velocity).

B. Boundary condition

As the next step we rewrite the boundary condition (12) for wave functions $\hat{f}_{\pm\mu}(s)$ defined at the trajectories s_1 and s_2 (see Fig. 2). Due to normal reflection of quasiparticles at the defect, the trajectories s_1 and s_2 with opposite momentum ($+\mu$ and $-\mu$) directions are coupled. Substituting the expressions (16) and (17) into the boundary condition (12), we obtain the relation between the amplitudes of incident $\hat{f}_{\pm\mu i}(s)$ and transmitted $\hat{f}_{\pm\mu t}(s)$ two-component quasiparticle wave functions at the point $s_0 = -b/\tan \theta_p$ where the trajectories cross the barrier,

$$(\eta + i) \hat{f}_{\pm\mu t} = \eta \hat{f}_{\pm\mu i} - i e^{\mp i\hat{\sigma}_z \theta_p} \hat{f}_{\mp\mu i}, \quad (27)$$

where $\eta = \sin \theta_p / Z$. Our further analysis of quasiparticle excitations is based on the solutions (21) and (22), which must be supplemented by the boundary conditions (27).

III. SPECTRUM OF THE VORTEX PINNED BY PLANAR DEFECT

We now proceed with the analysis of the subgap spectrum for a singly quantized vortex trapped by the planar defect. Hereafter in this section we assume the angular momentum to be positive, i.e., $\mu > 0$. The form of the two-component quasiparticle wave functions $\hat{f}_{\pm\mu}(s)$ depends on a position of the point s_0 at the trajectory. If the coordinate $s_0 \geq 0$ then the general solution (21) and (22) takes the form

$$\hat{f}_{\pm\mu}(s) = \begin{cases} c_{\pm\mu i} e^{i(\hat{\sigma}_z \mp 1)\pi/4} e^{-|K_{\mu}(s)|} \hat{\lambda}, & s \leq 0 \\ c_{\pm\mu i} e^{i(\hat{\sigma}_z \mp 1)\pi/4} (e^{-|K_{\mu}(s)|} - i\gamma_{\pm\mu} \hat{\sigma}_z e^{|K_{\mu}(s)|}) \hat{\lambda}, & 0 \leq s \leq s_0 \\ c_{\pm\mu t} e^{i(\hat{\sigma}_z \mp 1)\pi/4} e^{-|K_{\mu}(s)|} \hat{\lambda}, & s \geq s_0, \end{cases} \quad (28)$$

where

$$\gamma_{+\mu} = -\frac{\Lambda_\mu}{\Delta_0}(|\varepsilon_\mu| + \varepsilon), \quad \gamma_{-\mu} = \frac{\Lambda_\mu}{\Delta_0}(|\varepsilon_\mu| - \varepsilon).$$

Otherwise, if $s_0 \leq 0$,

$$\hat{f}_{\pm\mu}(s) = \begin{cases} c_{\pm\mu i} e^{i(\hat{\sigma}_z \mp 1)\pi/4} e^{-|K_\mu(s)|\hat{\lambda}}, & s \leq s_0 \\ c_{\pm\mu r} e^{i(\hat{\sigma}_z \mp 1)\pi/4} (e^{-|K_\mu(s)|} + i\gamma_{\pm\mu} \hat{\sigma}_z e^{|K_\mu(s)|}) \hat{\lambda}, & s_0 \leq s \leq 0 \\ c_{\pm\mu t} e^{i(\hat{\sigma}_z \mp 1)\pi/4} e^{-|K_\mu(s)|\hat{\lambda}}, & s \geq 0. \end{cases} \quad (29)$$

The unknown coefficients $c_{\pm\mu i}$ and $c_{\pm\mu t}$ in (28) and (29) are determined by the boundary conditions (27). The eigenfunctions $\hat{f}_{\pm\mu}(s)$ have to be normalized such that

$$\int_{-\infty}^{\infty} ds [|\hat{f}_{+\mu}(s)|^2 + |\hat{f}_{-\mu}(s)|^2] = k_\perp.$$

Substituting the expressions (28) or (29) into the boundary conditions (27), we obtain the following system of algebraic equations with respect to the amplitude $c_{\pm\mu i}$ of the incident waves:

$$\eta\gamma_{+\mu}c_{+\mu i} + (\gamma_{\mp\mu} \cos\theta_p + e^{-2K_0} \sin\theta_p)c_{-\mu i} = 0, \quad (30a)$$

$$\eta\gamma_{-\mu}c_{-\mu i} - (\gamma_{\pm\mu} \cos\theta_p - e^{-2K_0} \sin\theta_p)c_{+\mu i} = 0. \quad (30b)$$

The case $s_0 \geq 0$ ($s_0 < 0$) corresponds to the choice of upper (lower) sign in Eqs. (30), $K_0 = K_\mu(s_0)$, and the angle θ_p defines the direction of the ray with the angular momentum $+\mu$. To find the subgap quasiparticle excitation spectrum we should find the determinant of the algebraic system, and its zero gives us the equation for the energy spectrum ε :

$$\varepsilon^2(b, \theta_p) = \varepsilon_\mu^2 + \left(\frac{\Delta_0}{\Lambda_\mu}\right)^2 \frac{e^{-2K_0}}{\eta^2 + \cos^2\theta_p} \times \left[\Lambda_\mu \frac{|\varepsilon_\mu|}{\Delta_0} |\sin(2\theta_p)| + e^{-2K_0} \sin^2\theta_p \right]. \quad (31)$$

Clearly, the above expression describes the crossover to the standard CdGM spectrum in the limit of vanishing barrier strength ($\eta \rightarrow \infty$). Figure 4 shows the anomalous spectral branches as functions of the impact parameter $b = -\mu/k_F$ for different values of the dimensionless barrier strength Z and the trajectory directions in the x - y plane determined by the angle θ_p . The qualitative behavior of the spectrum is weakly sensitive to the concrete profile of the gap amplitude inside the core and we choose a simple model dependence

$$\delta_v(r) = r/\sqrt{r^2 + \xi^2}, \quad (32)$$

neglecting thus the influence of the defect on the behavior of the gap profile. Contrary to the CdGM case, the spectrum branch (31) does not cross the Fermi level in the presence of the defect. For rather small Z the minigap in the quasiparticle spectrum

$$\Delta_m(\theta_p) = \varepsilon(0, \theta_p) = \frac{\Delta_0}{\Lambda_0} \frac{Z}{\sqrt{1 + Z^2/\tan^2\theta_p}}$$

appears to be almost independent of θ_p in a wide range of angles except the small angular intervals close to $\theta_p = 0$ and $\theta_p = \pi$. It is natural to expect that in the patterns of the local

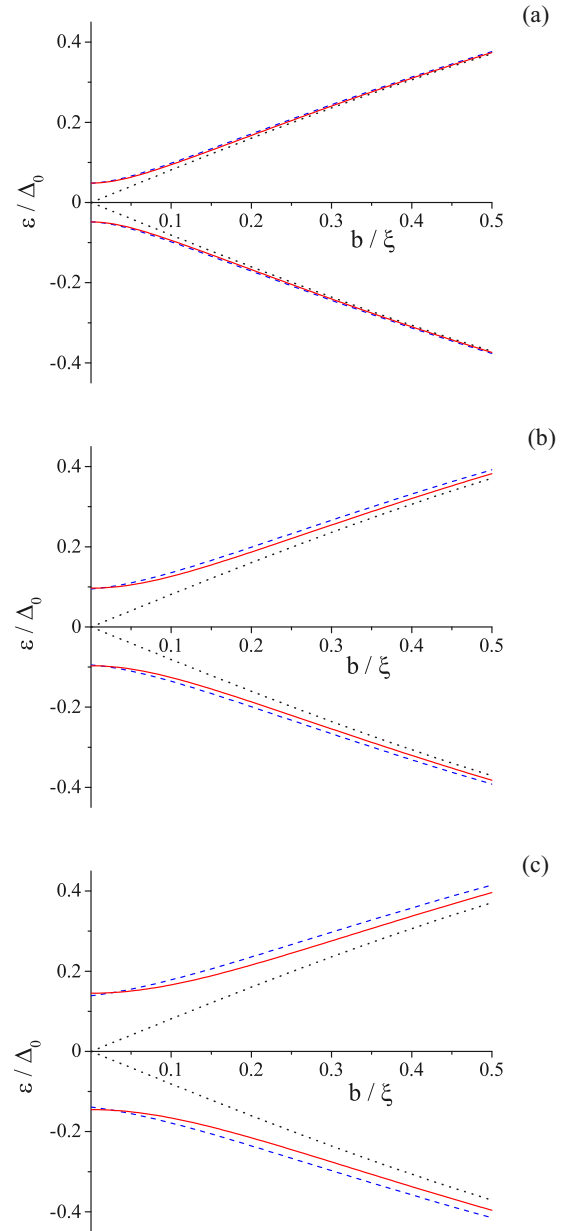


FIG. 4. Quasiparticle spectra $\varepsilon(b, \theta_p)$ calculated using Eq. (31) for different values of the dimensionless barrier strength Z and the trajectory direction θ_p in the x - y plane ($k_z = 0$): (a) $Z = 0.1$, (b) $Z = 0.2$, and (c) $Z = 0.3$. Dotted lines for $\theta_p = 0$ correspond to the CdGM branch of the spectrum. The blue dashed lines show the dependence for $\theta_p = \pi/4$ and the red solid lines show the dependence for $\theta_p = \pi/2$.

density of states (LDOS) this angular independent quantity should reveal itself as a soft gap $\Delta_{\text{soft}} \sim Z\Delta_0$ growing with the increasing barrier strength Z (see Sec. IV). We emphasize here the fact that this gap is soft since the spectrum (31) for small $|\tan\theta_p| \lesssim Z$ is gapless and thus these angular intervals can contribute to the LDOS at the Fermi level. This nonzero contribution exists of course only in the quasiclassical limit when we completely neglect the quantum mechanical nature of the trajectory precession which should be responsible for the opening of the hard minigap for the energies below Δ_{soft} .

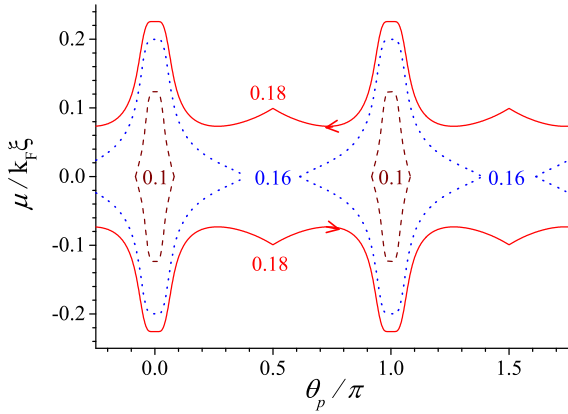


FIG. 5. Quasiparticle orbits in the μ - θ_p plane corresponding to different energy levels for the dimensionless barrier strength $Z = 0.3$. The numbers near the curves denote the corresponding values of ε/Δ_0 . The direction of trajectory precession along the orbits is shown by an arrow. We set here $k_z = 0$.

To derive the corresponding quantization rules in the limit $Z \ll 1$ we consider isoenergetic lines $\mu(\theta_p) = -k_\perp b(\theta_p)$ in the μ - θ_b plane. The resulting classical orbits are shown in Fig. 5. Generally, one can distinguish two types of the isoenergetic lines behavior. If the quasiparticle energy is of the order of the minigap ($\varepsilon \lesssim \Delta_{\text{soft}}$) there appear prohibited angular domains centered at the points $\theta_p = \pm\pi/2$ due to the normal reflection of quasiparticles at the defect. In this case classical orbits form close paths in μ - θ_b space corresponding to the precession of the trajectory in the region with the width $2\delta\theta_p(\varepsilon)$ near the points $\theta_p = 0, \pm\pi$. The width $2\delta\theta_p$ of the precession region grows with an increase in energy level. For small $|\mu| \ll k_\perp \xi$ the value $\delta\theta_p$ can be estimated as follows:

$$\delta\theta_p \simeq \frac{\varepsilon \Lambda_0 / \Delta_0}{\sqrt{1 - (\varepsilon \Lambda_0 / Z \Delta_0)^2}}. \quad (33)$$

Shrinking of the prohibited angular domains and the crossover from the closed orbits to the open ones occur at the energy ε^* satisfying the condition $\delta\theta_p(\varepsilon^*) = \pi/2$.

The low-lying energy levels of quasiparticles can be obtained by applying the Bohr-Sommerfeld quantization rule (9) for closed paths in the plane of canonically conjugate variables μ and θ_p . Figure 6 shows the typical dependence $\Sigma(\varepsilon)$ calculated using the spectrum (31). Taking $\varepsilon_\mu \simeq -\hbar\omega_0\mu$ for small μ values and replacing the real classical orbits in the μ - θ_b plane by the model one (see the inset in Fig. 6), one can obtain a reasonable fit (dashed curve) to the numerical results (solid curve):

$$\Sigma(\varepsilon) \approx 2 \frac{\varepsilon}{\hbar\omega_0} \delta\theta_p = \frac{2\varepsilon^2 \Lambda_0 / \Delta_0}{\hbar\omega_0 \sqrt{1 - (\varepsilon \Lambda_0 / Z \Delta_0)^2}}. \quad (34)$$

The above relation together with the Bohr-Sommerfeld rule (9) results in the explicit expression for discrete subgap energy levels

$$\begin{aligned} \varepsilon_n &\simeq \frac{\Delta_0 Z}{\Lambda_0} [p_n \sqrt{1 + p_n^2/4} - p_n^2/2]^{1/2}, \\ p_n &= \frac{\pi \Lambda_0 \Delta_0}{2E_F Z^2} (n + \beta), \end{aligned} \quad (35)$$

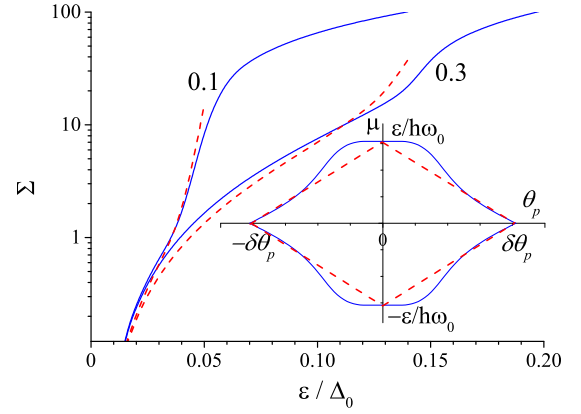


FIG. 6. Dependence $\Sigma(\varepsilon)$ (9) for two values of the dimensionless barrier strength $Z = 0.1; 0.3$. Results of numerical calculations are shown by the blue solid lines. Red dashed curves show approximate values of $\Sigma(\varepsilon)$ obtained from Eq. (34). The inset shows the quasiparticle orbit in the μ - θ_b plane (blue solid line) and its approximation (red dashed line) described by Eq. (34). We set here $k_z = 0$ and $E_F/\Delta_0 = 50$.

which appears to be justified for $\varepsilon_n/\Delta_0 \lesssim Z^2 \ll 1$. The expression (35) can be strongly simplified provided $p_n \ll 1$ for low-lying energy levels:

$$\varepsilon_n^2 \simeq \frac{\pi}{2\Lambda_0} \frac{\Delta_0^3}{E_F} (n + \beta) \left[1 - \frac{\pi \Lambda_0 \Delta_0}{4E_F Z^2} (n + \beta) \right].$$

The main term of the preceding relation appears to be in good agreement with the estimate (10) and describes qualitatively the behavior of spectrum of subgap quasiparticle states ($\varepsilon_n \sim n^{1/2}$) gliding along the planar defect. Both the hard minigap $\varepsilon_0 \lesssim \Delta_0 \sqrt{\Delta_0}/E_F \ll \Delta_{\text{soft}}$ in the discrete spectrum (35) and the interlevel spacing $\hbar\omega = \varepsilon_n - \varepsilon_{n-1}$ grow with the increase in the barrier strength Z . The wave functions of these gliding states are given by the expressions (28) and (29) describing the mixtures of the wave functions u and v with almost equal probabilities to find the quasiparticle in the electronlike and holelike states.

Besides its fundamental interest, the problem of a pinned vortex spectrum is important for understanding the nature of dissipation in the presence of planar defects. In particular, according to the spectral flow theory [18,26], it is the behavior of the anomalous branch which determines the high-frequency conductivity and Kerr effect [30,32]. As a result, the quasiparticle subgap spectrum can be tested by the measurements of the conductivity tensor at finite frequencies. The additional complication at this point arises from the obvious fact that the vortex during its motion under the effect of the Lorentz force can shift from the defect plane. Thus, the quantitative description of the appropriate response requires strictly speaking the solution of the problem for a shifted vortex. Still, the increase in the minigap obtained in our work indicates at least qualitatively that the spectral flow for a moving vortex should be suppressed according to very general arguments [18,26]. Thus, one can expect that the opening of the hard minigap ε_0 in the discrete quasiparticle spectrum (35) and change in the slope $\varepsilon(\mu)$ dependence (31) can cause the suppression of the dissipation accompanying the vortex motion and the

appropriate changes in the relation between the Ohmic and Hall conductivities (an increase in the Hall part of the AC response compared to the Ohmic one).

IV. LOCAL DENSITY OF STATES FOR A PINNED VORTEX

We now proceed with the calculations of the local density of states for a singly quantized vortex pinned at the planar defect. This quantity is known to be directly probed in the scanning tunneling microscopy and spectroscopy experiments [17]. For the sake of simplicity we assume here the Fermi surface to be a cylinder and neglect the dependence of the quasiparticle energy on the momentum component k_z along the cylinder axis z considering the motion of quasiparticles only in the x - y plane. The peculiarities of the LDOS are usually determined from the analysis of the local differential conductance (LDC)

$$\frac{dI/dV}{(dI/dV)_N} = \int_{-\infty}^{\infty} d\varepsilon \frac{N(\mathbf{r}, \varepsilon)}{N_0} \frac{\partial f(\varepsilon - eV)}{\partial V}, \quad (36)$$

where $(dI/dV)_N$ is the conductance of the normal metal junction and $f(\varepsilon) = 1/[1 + \exp(\varepsilon/T)]$ is a Fermi function. The expression (36) describes the two-dimensional map of the tunneling conductance $dI/dV(x, y)$ at an arbitrary bias voltage V between the STM tip and the sample surface.

Within the quasiclassical approach the LDOS

$$N(\mathbf{r}, \varepsilon) = k_F \int db |u_b(\mathbf{r})|^2 \delta(\varepsilon - \varepsilon(b)) \quad (37)$$

can be expressed through the electron component $u_b(r, \theta)$ of quasiparticle eigenfunctions (14) corresponding to the energy $\varepsilon(b, \theta_p)$ determined by Eqs. (23)–(26) and (31). The wave function $\hat{\Psi}(r, \theta)$ parametrized by the impact parameter $b = -\mu/k_F$,

$$\begin{aligned} \hat{\Psi}(r, \theta) &= \begin{pmatrix} u_b(r, \theta) \\ v_b(r, \theta) \end{pmatrix} \\ &= e^{i(2\mu + \hat{\sigma}_z)\theta/2} \int_0^{2\pi} \frac{d\alpha}{2\pi} e^{ik_F r \cos \alpha + i(2\mu + \hat{\sigma}_z)\alpha/2} \hat{f}_\mu(r \cos \alpha), \end{aligned} \quad (38)$$

in the limit $k_F r \gg 1$ can be evaluated using the stationary phase method. For an impact parameter $|b| \leq r$ the stationary phase points are given by the condition $\sin \alpha_{1,2} = -b/r$. Summing over two contributions in the vicinity of the stationary angles $\alpha_1 = \theta_{p1} - \theta = \alpha_r$ and $\alpha_2 = \theta_{p2} - \theta = \pi - \alpha_r$, we can write the electron component $u_b(r, \theta)$ of quasiparticle eigenfunctions as

$$\begin{aligned} u_b(r, \theta) &= \left(\frac{1}{2\pi k_F s_r} \right)^{1/2} e^{i(2\mu+1)\theta/2} \\ &\quad \times [f_\mu^u(s_r) e^{i\varphi_r} + f_\mu^u(-s_r) e^{-i\varphi_r + i(2\mu+1)\pi/2}], \end{aligned} \quad (39)$$

where $s_r = r|\cos \alpha_r| = \sqrt{r^2 - b^2}$. The phase

$$\varphi_r = k_F r \cos \alpha_r + |\mu| \alpha_r + \text{sgn}(\mu) \alpha_r / 2 - \pi / 4$$

is determined by the trajectory orientation angle $\alpha_r = -\arcsin(b/r)$. Neglecting the oscillations at the atomic length scale, we obtain the slowly varying envelope

function

$$|u_b(r, \theta)|^2 \simeq \frac{1}{2\pi k_F s_r} [|f_\mu^u(s_r)|^2 + |f_\mu^u(-s_r)|^2], \quad (40)$$

where the function $f_\mu^u(\pm s_r)$ is determined by the relations (28) or (29).

We have calculated the differential conductance using Eqs. (36), (37), and (40) for low temperature $T/\Delta_0 = 0.02$ for different values of the dimensionless barrier strength Z . The typical examples of dependence of the local differential conductance dI/dV vs the bias voltage eV at various distances r from the vortex axis are shown in Fig. 7. In order to compare our results with the standard CdGM ones, we present the dependence of the local dI/dV vs voltage at different distances r from the Abrikosov vortex axis in the absence of the barrier ($Z = 0$). One can clearly observe the disappearance of the zero-bias peak in the core ($r = 0$) and opening of the soft spectral minigap Δ_{soft} caused by the normal scattering at the defect [Fig. 7(a)]. The barrier results in the anisotropy of the LDC structure in the x - y plane [Figs. 7(b) and 7(c)]. The anisotropy of the LDC grows when barrier strength Z increases. Figure 8 illustrates the evolution of the local differential conductance $dI/dV(eV, x, y)$ distribution in the x - y plane for several values of the bias voltage V and dimensionless barrier strength Z . In Figs. 8(a) and 8(b) we can see the spread of the zero-bias peak along the defect, which appears to be another hallmark of the crossover from the Abrikosov to the Josephson vortex type. Due to the normal reflection of electrons and holes at the defect plane, we get the azimuthal modulation of the LDC developing with the growth of the barrier strength Z .

V. SUMMARY

We have investigated the transformation of the subgap spectrum of quasiparticle excitations in the Abrikosov vortex pinned by the planar defect with a high transparency. We found that the normal scattering at the defect surface results in the opening of a soft minigap Δ_{soft} in the elementary excitation spectrum near the Fermi level. The minigap size grows with the decrease in the transparency of the barrier. The increase in the resulting soft gap affects the splitting of the zero-bias anomaly in the tunneling spectral characteristics and perturb the circular symmetry of the LDOS peaks. The normal reflection of electrons and holes at the defect plane changes the topology of the isoenergetic orbits in μ - θ_p space. This topological transition revealed in the specific behavior of the quantized quasiparticle levels and density of states can be considered as a hallmark of the crossover from the Abrikosov to the Josephson vortex. As a result, there appears a different type of subgap quasiparticle states gliding along the defect, which reveal the qualitatively different behavior of the discrete spectrum $\varepsilon_n \sim n^{1/2}$. The hard minigap $\varepsilon_0 \ll \Delta_{\text{soft}}$ in the spectrum of energy levels exceeds noticeably the value of the CdGM minigap $\hbar\omega_0 \ll \varepsilon_0$. The decrease in the barrier transparency is accompanied by the increase in the hard minigap ε_0 in the spectrum which can be observed in the measurements of the Ohmic and Hall conductivities at finite frequencies. The basic properties of the vortex such as pinning and mobility along the defect plane are strongly affected by

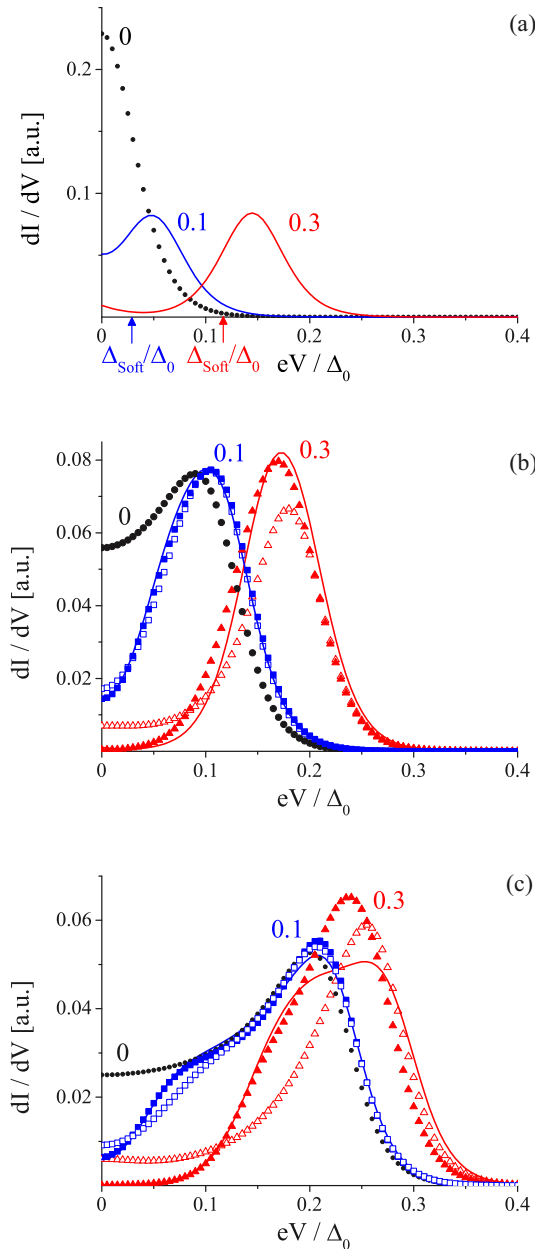


FIG. 7. Local differential conductance dI/dV versus bias voltage eV at different points r and θ on the x - y plane: (a) $r = 0$, (b) $r = 0.14\xi$, and (c) $r = 0.28\xi$. The numbers near the curves are the corresponding values of the dimensionless barrier strength Z . The lines correspond to the case $\theta = \pi/4$, open symbols $\theta = 0$, and closed symbols $\theta = \pi/2$. We set here $T/\Delta_0 = 0.02$. For reference, black closed circles show the local dI/dV curves for the free Abrikosov vortex ($Z = 0$). The soft minigap Δ_{soft} corresponding to the maximal slope of the energy dependence of the LDOS is indicated by the arrows in (a).

these changes in the orbit topology. We have also analyzed the distinctive features of the quasiparticle density of states, which accompany the transformation of the subgap quasiparticle spectrum and the topology of the isoenergetic orbits for an Abrikosov vortex pinned by a planar defect with a perfect boundary. One can expect, however, that barrier imperfections and roughness should result in a partial smearing of both the

hard and soft gap features similarly to the effect of the point impurity scattering.

As for the transformation of the shape of the vortex core, it is of course related to the changes in the low-energy spectrum since the latter cause the change in both the supercurrent density and gap profile. At high barrier transparency $\mathcal{T} \gtrsim \mathcal{T}_\xi$ we see that the appearance of the nutating states strongly suppresses the DOS below the soft minigap $\Delta_{\text{soft}} \sim Z\Delta_0$, which should result in the partial increase in the gap value inside the core. Without the self-consistent calculations we can only assume that a further decrease in the barrier transparency fully suppresses the quasiparticle states nutating around the direction parallel to the barrier and only the high-energy states close to the gap can survive. Such suppression of the low-energy DOS obviously gives the disappearance of the normal vortex core.

Finally, we note that recently the vortices pinned by the defects were proposed as the hosts for the Majorana states in the systems consisting of a primary superconductor with conventional pairing and a low-dimensional layer with a nontrivial topology [s -wave superconductors with a cylindrical hole (cavity) deposited on the surface of a topological insulator (TI)] [51–54]. An Abrikosov vortex pinned by the hole generates a “pancake” vortex inside 2D topological superconductor induced in TI due to proximity. Such a pancake is known to support a Majorana fermion state bound to the vortex core [55,56]. The isolating inclusions or cavity in the vortex core in the primary superconductor allow a shift of the low-energy core spectrum from the Fermi level, improving the topological protection (robustness) of the Majorana states in the 2D topological superconductor. The vortex at the planar defect considered in our work can provide a perspective platform for such states since the hard minigap in the core can exhibit a strong increase even in the limit of the defect with high transparency when the shape of the gap inside the vortex core is only weakly perturbed by the scattering. The planar defect removes the low-lying CdGM states from the vortex core and provides the robustness of the Majorana states. Another advantage of this geometry (see Fig. 9) is related to the possibility to move the vortices along the defects, changing thus the positions of the Majorana states in the attached 2D layer without changing the minigap responsible for the desired topological protection.

ACKNOWLEDGMENTS

We thank A. I. Buzdin, Ya. V. Fominov, V. B. Geshkenbein, A. Bezryadin, and A. A. Bespalov for stimulating discussions. This work was supported in part by the Russian Foundation for Basic Research under Grants No. 18-42-520037 and No. 19-31-51019, and the Foundation for the Advancement of Theoretical Physics and Mathematics “BASIS” Grant No. 18-1-2-64-2. The work on the LDOS calculations was supported by Russian Science Foundation (Grant No. 20-12-00053).

APPENDIX: ANDREEV EQUATIONS

The BdG equations for particlelike u and holelike v parts of the two-component quasiparticle wave

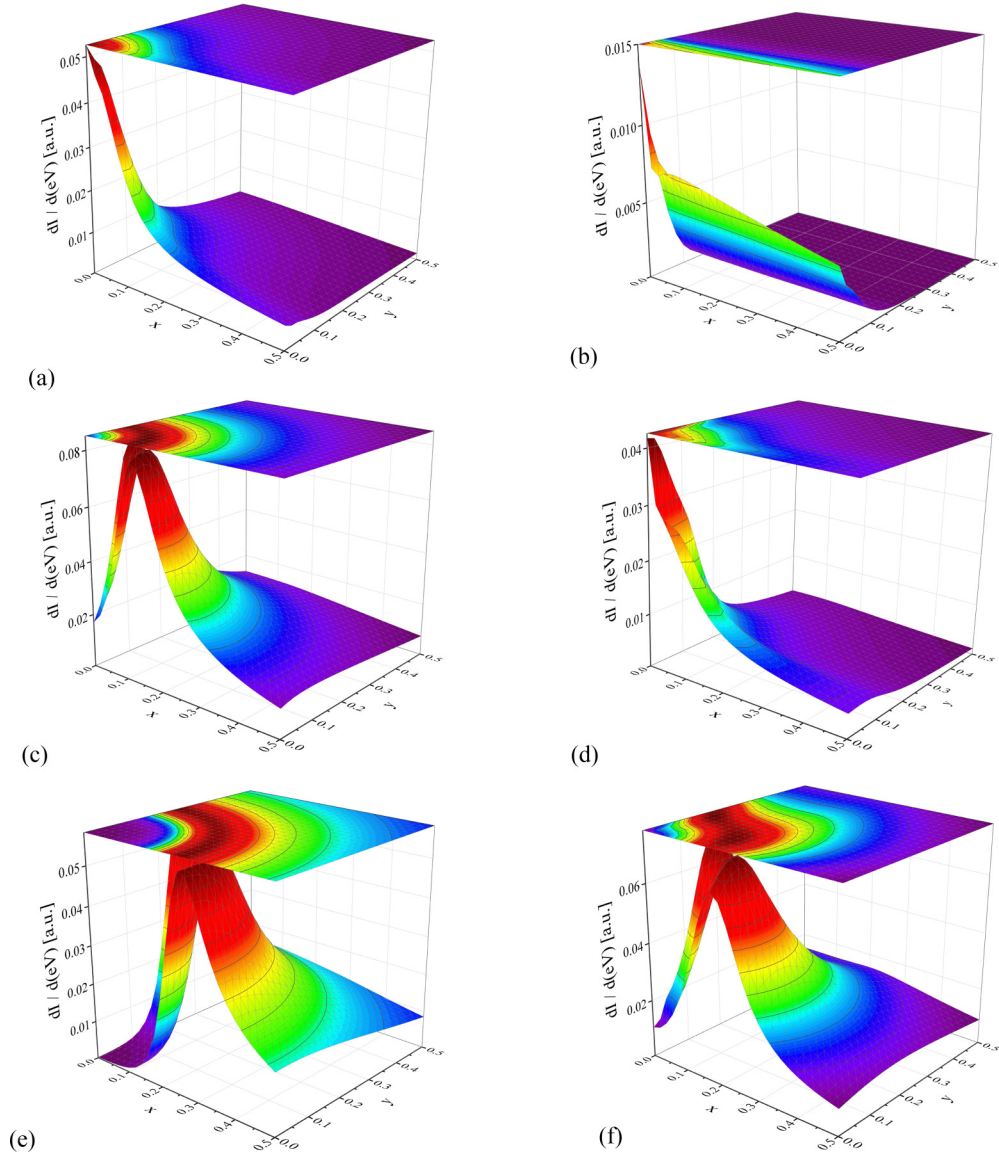


FIG. 8. Evolution of the local differential conductance $dI/dV(eV, x, y)$ corresponding to different bias voltages (a) and (b) $eV = 0$, (c) and (d) $eV/\Delta_0 = 0.1$, and (e) and (f) $eV/\Delta_0 = 0.2$ for different values of the dimensionless barrier strength Z : (a), (c), and (e) $Z = 0.1$ and (b), (d), and (f) $Z = 0.3$. We set here $T/\Delta_0 = 0.02$.

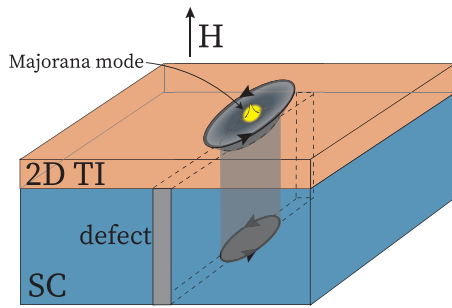


FIG. 9. Possible setup of the Majorana-type system based on the vortex pinned by a planar defect. A robust Majorana fermion can be localized inside the vortex core created on the surface of the topological insulator (TI) by the proximity effect to the primary s -wave superconductor (SC).

functions $(U, V)^T = (u(\mathbf{r}), v(\mathbf{r}))^T \exp(ik_z z)$ have the following form:

$$-\frac{\hbar^2}{2m}(\nabla^2 + k_{\perp}^2)u + \Delta(\mathbf{r})v = \epsilon u, \quad (\text{A1a})$$

$$\frac{\hbar^2}{2m}(\nabla^2 + k_{\perp}^2)v + \Delta^*(\mathbf{r})u = \epsilon v. \quad (\text{A1b})$$

Here $\nabla = \partial_x \mathbf{x}_0 + \partial_y \mathbf{y}_0$, $\mathbf{r} = (x, y)$ is a radius vector in the plane perpendicular to the magnetic field direction, $\Delta(\mathbf{r})$ is the gap function, and $k_{\perp}^2 = k_F^2 - k_z^2$. We assume the system to be homogeneous along the z axis; thus the $\hbar k_z$ projection of the momentum is conserved and we restrict our analysis to the case of the weak external magnetic field and the extreme type-II superconductors where the vector potential \mathbf{A} can be neglected.

The two-component wave function $\hat{\Psi} = (u(\mathbf{r}), v(\mathbf{r}))^T$ in the momentum representation can be written as

$$\hat{\Psi}(\mathbf{r}) = \frac{1}{(2\pi\hbar)^2} \int_{-\infty}^{+\infty} d^2\mathbf{p} e^{i\mathbf{p}\mathbf{r}/\hbar} \hat{\psi}(\mathbf{p}), \quad (\text{A2})$$

where $\mathbf{p} = p(\cos\theta_p, \sin\theta_p) = p\mathbf{p}_0$ defines the polar coordinate system in momentum space. The unit vector $\mathbf{p}_0 = (\cos\theta_p, \sin\theta_p)$ is parametrized by the angle θ_p , which determines the trajectory direction in the x - y plane. The coordinate operator in the polar coordinate system (p, θ_p) can be written as

$$\hat{\mathbf{r}} = i\hbar \frac{\partial}{\partial \mathbf{p}} = i\hbar \left(\mathbf{p}_0 \frac{\partial}{\partial p} + \frac{i}{p} [\mathbf{z}_0, \mathbf{p}_0] \hat{\mu} \right), \quad (\text{A3})$$

where the operator of z projection of angular momentum $\hat{\mu}$ is given by the expression

$$\hat{\mu} = \frac{1}{\hbar} [\mathbf{r}, \mathbf{p}] \mathbf{z}_0 = -i \frac{\partial}{\partial \theta_p}. \quad (\text{A4})$$

Within the quasiclassical approach the characteristic length scale of envelopes of quasiparticle waves is determined by the superconducting coherence length ξ , and the quasiparticle wave function can be viewed as a wave packet with momentum absolute values close to $\hbar k_{\perp}$ since $k_F \xi \gg 1$ is assumed. Therefore, we look for solutions with absolute values \mathbf{p} close to the value $\hbar k_{\perp}$: $p = \hbar k_{\perp} + q$ ($q \ll \hbar k_{\perp}$). In this case one can obtain the expression for the coordinate operator

$$\hat{\mathbf{r}} = i\hbar \mathbf{p}_0 \frac{\partial}{\partial q} + \frac{i}{2k_{\perp}} \left\{ [\mathbf{z}_0, \mathbf{p}_0], \frac{\partial}{\partial \theta_p} \right\}, \quad (\text{A5})$$

where $\{\dots\}$ is an anticommutator. Let us now introduce a Fourier transformation

$$\hat{\psi}(\mathbf{p}) = \frac{1}{k_{\perp}} \int_{-\infty}^{+\infty} ds e^{-iqs/\hbar} \hat{\psi}(s, \theta_p), \quad (\text{A6})$$

where $s = r \cos(\theta_p - \theta)$ is a coordinate along a quasiclassical trajectory, which is a straight line along the direction of the quasiparticle momentum \mathbf{p} . The trajectory orientation angle is given by the θ_p value. The wave function $\hat{\Psi}(\mathbf{r})$ in the polar coordinate system (r, θ) can be found from Eqs. (A2)

and (A6):

$$\hat{\Psi}(r, \theta) = \int_0^{2\pi} e^{ik_{\perp} r \cos(\theta_p - \theta)} \hat{\psi}(r \cos(\theta_p - \theta), \theta_p) \frac{d\theta_p}{2\pi}, \quad (\text{A7})$$

where functions $\hat{\psi}(s, \theta_p)$ vary slowly at the trajectory θ_p . The expression for the coordinate operator (A5) in the (s, θ_p) representation reads

$$\hat{\mathbf{r}} = s\mathbf{p}_0 + \frac{i}{2k_{\perp}} \left\{ [\mathbf{z}_0, \mathbf{p}_0], \frac{\partial}{\partial \theta_p} \right\}. \quad (\text{A8})$$

Then the BdG equations (A1) in the (s, θ_p) representation take the form

$$\begin{aligned} \hat{H} \hat{\psi}(s, \theta_p) &= \epsilon \hat{\psi}(s, \theta_p), \\ \hat{H} &= -i\hat{\sigma}_z \frac{\hbar^2 k_{\perp}}{m} \frac{\partial}{\partial s} + \begin{bmatrix} 0 & \Delta(\hat{\mathbf{r}}) \\ \Delta^*(\hat{\mathbf{r}}) & 0 \end{bmatrix}, \end{aligned} \quad (\text{A9})$$

where $\hat{\sigma}_x$, $\hat{\sigma}_y$, and $\hat{\sigma}_z$ are the Pauli matrices. Considering the eikonal approximation for the angular dependence of the wave function

$$\hat{\psi}(s, \theta_p) = e^{iS_e(\theta_p)} \hat{f}(s, \theta_p),$$

where

$$-\frac{1}{k_{\perp}} \frac{\partial S_e}{\partial \theta_p} = b(\theta_p)$$

is an impact parameter of a quasiclassical trajectory, and assuming a rather slow angular dependence of $\hat{f}(s, \theta_p)$ [$\hat{f}(s, \theta_p) \simeq \hat{f}_{\mu}(s)$], one can neglect a differential operator $\partial/\partial \theta_p$ in the Hamiltonian (A9). The function $\hat{f}_{\mu}(s)$ satisfies the Andreev equations along the quasiclassical trajectory with a certain orientational angle θ_p and impact parameter $b = -\mu/k_{\perp}$,

$$\begin{aligned} -i\hat{\sigma}_z \frac{\hbar^2 k_{\perp}}{m} \frac{\partial \hat{f}_{\mu}}{\partial s} + \hat{\sigma}_x \text{Re} \Delta(x, y) \hat{f}_{\mu} \\ - \hat{\sigma}_y \text{Im} \Delta(x, y) \hat{f}_{\mu} &= \epsilon \hat{f}_{\mu}, \end{aligned} \quad (\text{A10})$$

where

$$x = s \cos \theta_p - b \sin \theta_p, \quad y = s \sin \theta_p + b \cos \theta_p.$$

Changing the sign of the coordinate s , one can observe a useful symmetry property of the solution of Eq. (A10):

$$\hat{f}_{\mu}(-s) = \pm \hat{\sigma}_y \hat{f}_{\mu}(s).$$

-
- [1] A. A. Abrikosov, Zh. Eksp. Teor. Fiz. **32**, 1442 (1957) [Sov. Phys. JETP **5**, 1174 (1957)].
- [2] A. Barone and G. Paterno, *Physics and Applications of the Josephson Effect* (Wiley, New York, 1982).
- [3] A. Gurevich, Phys. Rev. B **46**, 3187(R) (1992).
- [4] T. Horide, K. Matsumoto, A. Ichinose, M. Mukaida, Y. Yoshida, and S. Horii, Phys. Rev. B **75**, 020504(R) (2007).
- [5] T. Horide, K. Matsumoto, Y. Yoshida, M. Mukaida, A. Ichinose, and S. Horii, Phys. Rev. B **77**, 132502 (2008).
- [6] I. N. Khlyustikov and A. I. Buzdin, Adv. Phys. **36**, 271 (1987).
- [7] A. Gurevich, M. S. Rzchowski, G. Daniels, S. Patnaik, B. M. Hinaus, F. Carillo, F. Tafuri, and D. C. Larbalestier, Phys. Rev. Lett. **88**, 097001 (2002).
- [8] H. Hilgenkamp and J. Mannhart, Rev. Mod. Phys. **74**, 485 (2002).
- [9] C. Jooss, R. Warthmann, and H. Kronmüller, Phys. Rev. B **61**, 12433 (2000).
- [10] M. Djupmyr, G. Cristiani, H. U. Habermeier, and J. Albrecht, Phys. Rev. B **72**, 220507(R) (2005).
- [11] F. Tafuri and J. R. Kirtley, Rep. Prog. Phys. **68**, 2573 (2005).

- [12] A. A. Golubov, M. Y. Kupriyanov, and E. Il'ichev, *Rev. Mod. Phys.* **76**, 411 (2004).
- [13] H. F. Hess, R. B. Robinson, R. C. Dynes, J. M. Valles, Jr., and J. V. Waszczak, *Phys. Rev. Lett.* **62**, 214 (1989).
- [14] B. W. Hoogenboom, M. Kugler, B. Revaz, I. Maggio-Aprile, O. Fischer, and C. Renner, *Phys. Rev. B* **62**, 9179 (2000).
- [15] I. Guillamon, H. Suderow, S. Vieira, L. Cario, P. Diener, and P. Rodiere, *Phys. Rev. Lett.* **101**, 166407 (2008).
- [16] G. Karapetrov, J. Fedor, M. Iavarone, D. Rosenmann, and W. K. Kwok, *Phys. Rev. Lett.* **95**, 167002 (2005).
- [17] D. Roditchev, C. Brun, L. Serrier-Garcia, J. C. Cuevas, V. H. L. Bessa, M. V. Milošević, F. Debontridder, V. Stolyarov, and T. Cren, *Nat. Phys.* **11**, 332 (2015).
- [18] N. B. Kopnin, *Theory of Nonequilibrium Superconductivity* (Clarendon, Oxford, 2001).
- [19] F. Guinea and Y. Pogorelov, *Phys. Rev. Lett.* **74**, 462 (1995).
- [20] M. V. Feigel'man and M. A. Skvortsov, *Phys. Rev. Lett.* **78**, 2640 (1997).
- [21] A. I. Larkin and Y. N. Ovchinnikov, *Phys. Rev. B* **57**, 5457 (1998).
- [22] M. A. Skvortsov, D. A. Ivanov, and G. Blatter, *Phys. Rev. B* **67**, 014521 (2003).
- [23] A. S. Mel'nikov and A. V. Samokhvalov, *Pis'ma Zh. Eksp. Teor. Fiz.* **94**, 823 (2011) [*JETP Lett.* **94**, 759 (2011)].
- [24] C. Caroli, P. G. de Gennes, and J. Matricon, *Phys. Lett.* **9**, 307 (1964).
- [25] A. F. Andreev, *Zh. Eksp. Teor. Fiz.* **46**, 1823 (1964) [*Sov. Phys. JETP* **19**, 1228 (1964)].
- [26] G. E. Volovik, *The Universe in a Helium Droplet* (Clarendon, Oxford, 2003).
- [27] Y. Tanaka, S. Kashiwaya, and H. Takayanagi, *Jpn. J. Appl. Phys.* **34**, 4566 (1995).
- [28] M. Eschrig, D. Rainer, and J. A. Sauls, in *Vortices in Unconventional Superconductors and Superfluids*, edited by R. P. Huebener, N. Schopohl and G. E. Volovik, Springer Series in Solid-State Sciences Vol. 132 (Springer, Berlin, 2002), pp. 175–203.
- [29] A. S. Mel'nikov, A. V. Samokhvalov, and M. N. Zubarev, *Phys. Rev. B* **79**, 134529 (2009).
- [30] B. Rosenstein, I. Shapiro, E. Deutch, and B. Y. Shapiro, *Phys. Rev. B* **84**, 134521 (2011).
- [31] A. S. Mel'nikov, A. V. Samokhvalov, and V. L. Vadimov, *Pisma ZhETF* **102**, 886 (2015) [*JETP Lett.* **102**, 775 (2015)].
- [32] V. L. Vadimov and A. S. Mel'nikov, *J. Low Temp. Phys.* **183**, 342 (2016).
- [33] L. D. Landau and L. P. Pitaevskii, *Statistical Physics* (Pergamon, Oxford, 1980), Pt. 2, Chap. 5.
- [34] N. B. Kopnin, A. S. Mel'nikov, V. I. Pozdnyakova, D. A. Ryzhov, I. A. Shereshevskii, and V. M. Vinokur, *Phys. Rev. Lett.* **95**, 197002 (2005).
- [35] N. B. Kopnin, A. S. Melnikov, V. I. Pozdnyakova, D. A. Ryzhov, I. A. Shereshevskii, and V. M. Vinokur, *Phys. Rev. B* **75**, 024514 (2007).
- [36] A. S. Mel'nikov, D. A. Ryzhov, and M. A. Silaev, *Phys. Rev. B* **78**, 064513 (2008).
- [37] A. S. Mel'nikov, D. A. Ryzhov, and M. A. Silaev, *Phys. Rev. B* **79**, 134521 (2009).
- [38] I. M. Lifshitz, *Zh. Eksp. Teor. Fiz.* **38**, 1569 (1960) [*Sov. Phys. JETP* **11**, 1130 (1960)].
- [39] Y. M. Blanter, M. I. Kaganov, A. V. Pantsulaya, and A. A. Varlamov, *Phys. Rep.* **245**, 159 (1994).
- [40] G. E. Volovik, *Pis'ma Zh. Eksp. Teor. Fiz.* **49**, 343 (1989) [*JETP Lett.* **49**, 391 (1989)].
- [41] S. Mel'nikov and M. A. Silaev, *Pis'ma Zh. Eksp. Teor. Fiz.* **83**, 675 (2006) [*JETP Lett.* **83**, 578 (2006)].
- [42] C. W. J. Beenakker and H. van Houten, *Phys. Rev. Lett.* **66**, 3056 (1991); C. W. J. Beenakker, *ibid.* **67**, 3836 (1991).
- [43] N. B. Kopnin and G. E. Volovik, *Pis'ma Zh. Eksp. Teor. Fiz.* **64**, 641 (1996) [*JETP Lett.* **64**, 690 (1996)]; N. B. Kopnin, *Phys. Rev. B* **57**, 11775 (1998).
- [44] N. B. Kopnin and G. E. Volovik, *Phys. Rev. Lett.* **79**, 1377 (1997).
- [45] D. N. Basov, M. M. Fogler, A. Lanzara, F. Wang, and Y. Zhang, *Rev. Mod. Phys.* **86**, 959 (2014).
- [46] A. H. Castro Neto, F. Guinea, N. M. R. Peres, K. S. Novoselov, and A. K. Geim, *Rev. Mod. Phys.* **81**, 109 (2009).
- [47] B. Janko, *Phys. Rev. Lett.* **82**, 4703 (1999).
- [48] G. Blatter, M. V. Feigel'man, V. B. Geshkenbein, A. I. Larkin, and V. M. Vinokur, *Rev. Mod. Phys.* **66**, 1125 (1994).
- [49] G. E. Blonder, M. Tinkham, and T. M. Klapwijk, *Phys. Rev. B* **25**, 4515 (1982).
- [50] N. B. Kopnin, A. S. Mel'nikov, and V. M. Vinokur, *Phys. Rev. B* **68**, 054528 (2003).
- [51] A. L. Rakhmanov, A. V. Rozhkov, and F. Nori, *Phys. Rev. B* **84**, 075141 (2011).
- [52] P. A. Ioselevich and M. V. Feigel'man, *Phys. Rev. Lett.* **106**, 077003 (2011).
- [53] P. A. Ioselevich, P. M. Ostrovsky, and M. V. Feigel'man, *Phys. Rev. B* **86**, 035441 (2012).
- [54] R. S. Akzyanov, A. V. Rozhkov, A. L. Rakhmanov, and F. Nori, *Phys. Rev. B* **89**, 085409 (2014).
- [55] L. Fu and C. L. Kane, *Phys. Rev. Lett.* **100**, 096407 (2008).
- [56] J. D. Sau, R. M. Lutchyn, S. Tewari, and S. Das Sarma, *Phys. Rev. B* **82**, 094522 (2010).